ELSEVIER

Chemical vapor deposition of methane for single-walled carbon nanotubes

Jing Kong [a], Alan M. Cassell [a,b], Hongjie Dai [a,*]

[a] *Department of Chemistry, Stanford University, Stanford, CA 94305, USA*
[b] *NASA Ames Research Center, Moffett Field, CA 94035, USA*

Abstract

We report the synthesis of high-quality single-walled carbon nanotubes (SWNT) by chemical vapor deposition (CVD) of methane at 1000°C on supported Fe_2O_3 catalysts. The type of catalyst support is found to control the formation of individual or bundled SWNTs. Catalysts supported on crystalline alumina nanoparticles produce abundant individual SWNTs and small bundles. Catalysts supported by amorphous silica particles produce only SWNT bundles. Studies of the ends of SWNTs lead to an understanding of their growth mechanism. Also, we present the results of methane CVD on supported NiO, CoO and NiO/CoO catalysts. © 1998 Published by Elsevier Science B.V. All rights reserved.

1. Introduction

Significant progress was made recently in synthesizing gram quantities of single-walled carbon nanotubes (SWNT) [1] using laser-ablation [2] and arc-discharge methods [3,4]. Both methods involve the evaporation of carbon at ∼ 3000°C, with the synthesized SWNTs predominantly in the form of rope-like bundles [2–4]. Currently, several topics in SWNT synthesis still remain challenging. First, samples containing mostly defect-free individual SWNTs have yet to be obtained. Such samples are desired for fundamental studies of the physics in nanotubes [5]. Secondly, practical applications of nanotubes will require the synthesis of high-quality SWNT materials at a very large scale. These challenges could be met by developing CVD methods that utilize carbon-rich gases as carbon feedstock. CVD of various hydrocarbon gases on transition-metal catalysts has been successful in obtaining carbon fibers and multi-walled nanotubes [6–13]. The CVD methods are attractive because of their efficiency in generating carbon feedstock and the straightforward scale-up. Furthermore, it could be possible to gain control over the types of nanotubes grown by controlling various parameters that are involved in CVD experiments. Nevertheless, CVD approaches have not been fully explored to synthesize single-walled carbon nanotubes. So far, there are only two reported [14,15] CVD syntheses of SWNTs including the method that utilizes CO and supported MoO_x catalyst [14].

In this Letter, we report high-quality SWNT materials obtained by chemical-vapor deposition of methane on supported transition-metal oxide cata-

---

* Corresponding author. E-mail: hdai@chem.stanford.edu

Table 1
Summary of results of methane CVD experiments using supported metal-oxide catalysts

Catalyst composition	Support material	SWNTs?	Description of synthesized material
Fe_2O_3	alumina	yes	abundant individual SWNTs; some bundles; occasional double-walled tubes
Fe_2O_3	silica	yes	abundant SWNT bundles
CoO	alumina	yes	some SWNT bundles and individual SWNTs
CoO	silica	no	no tubular materials synthesized
NiO	alumina	no	mainly defective multi-walled structures with partial metal filling
NiO	silica	no	no tubular materials synthesized
NiO/CoO	alumina	no	no tubular materials synthesized
NiO/CoO	silica	yes	some SWNT bundles

lysts. Our general approach is similar to previous work in producing carbon fibers and multi-walled nanotubes. However, we find several factors that are key to producing single-walled carbon nanotubes. These factors include the choice of methane, catalyst composition and type of support.
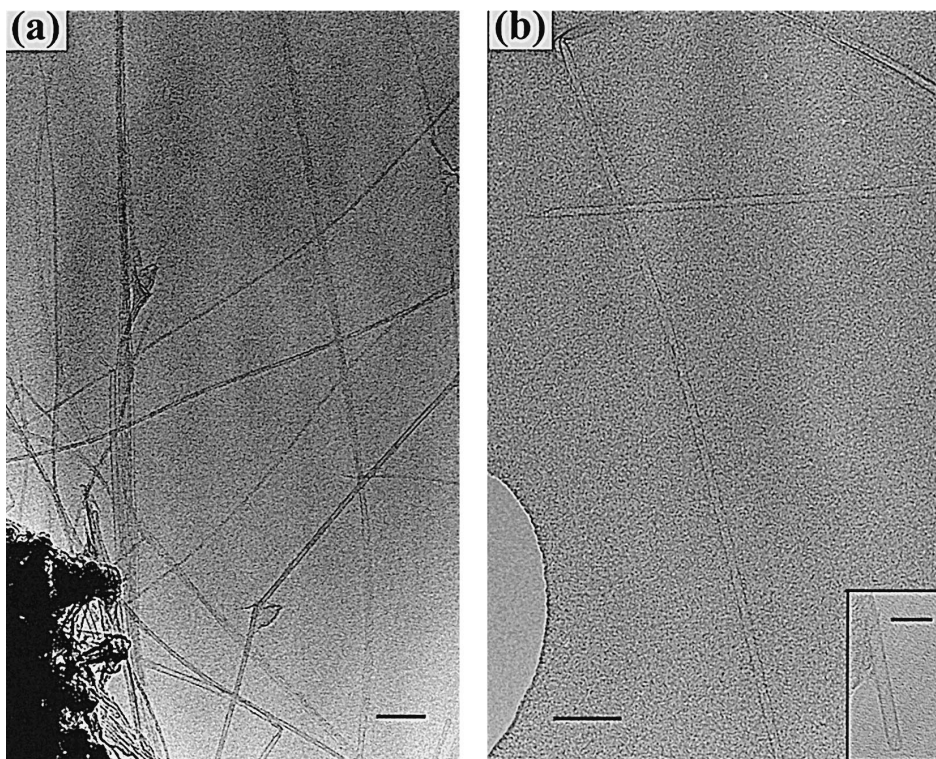

Fig. 1. (a) TEM image of individual and bundled SWNTs produced on the Fe_2O_3/alumina catalyst. Scale bar: 100 nm. (b) High-resolution TEM image of a $d = 5$ nm individual SWNT. Scale bar: 50 nm. Inset shows the dome-closed end of a $d = 3$ nm SWNT. Scale bar: 10 nm.

2. Experimental

The first step for our CVD synthesis is to prepare a supported catalyst. As an example, a Fe_2O_3 catalyst is prepared by impregnating 1 g of fumed-alumina (Degussa, 100 m^2/g surface area) nanoparticles with 30 ml of a methanol solution that contains 0.245 g of $Fe(NO_3)_3 \cdot 9H_2O$. The impregnation typically lasts for 1 h at room temperature. The methanol solution was then removed via rotary evaporation at 80°C. The material is then heated at 150°C overnight followed by grinding into a fine powder. This resulting catalyst is denoted as Fe_2O_3/alumina. In this work, the (metal-mol)/(alumina weight) ratio is 0.6 mmol/g and is fixed for all of the alumina supported metal-oxide catalysts (NiO, CoO and NiO/CoO mixture with 1:1 mol ratio). For all of the catalysts supported by fumed-silica (Degussa AEROSIL, 300 m^2/g), the (metal-mol)/(silica weight) ratio is kept at 0.9 mmol/g.

For a methane CVD experiment, ∼ 10 mg of the catalyst was placed in a quartz tube mounted in a tube furnace. An argon flow was passed through the quartz tube as the furnace was heated to reach 1000°C. The Ar flow was then replaced by methane (99% purity) at a flow rate of 6150 cm^3/min under 1.25 atm. head pressure. The methane flow lasted for 10 min and was replaced by argon and the furnace was cooled to room temperature. Samples for transmission electron microscopy were prepared by sonicating ∼ 2 mg of the synthesized material in 10 ml of methanol or 1,2-dichloroethane for half an hour. A few drops of the resulting suspension were then put onto a holey-carbon TEM grid. The TEM was operated at beam energies between 120 and 200 kV using a Philips CM20 instrument. For atomic force microscopy (AFM) studies, samples were prepared by allowing a drop of the suspension to evaporate on a freshly cleaved mica surface.

3. Results

We summarize our CVD syntheses in Table 1, and the overall result is that SWNTs are obtainable using methane CVD. In particular, with the Fe_2O_3/alumina catalyst, we obtained abundant individual SWNTs. Fig. 1a shows a TEM image of SWNTs synthesized with this catalyst. A high-mag-

nification TEM image is shown in Fig. 1b. By imaging several samples obtained under the same conditions, we measured that the individual SWNTs have diameters in ranges of 1.3–5.4 nm, and their lengths are up to 10 μm. In Fig. 2a, we present an AFM image of the nanotubes in this sample. The diameters of the nanotubes are determined from their topographic heights. Fig. 2b shows a statistical diameter histogram obtained from AFM data by measuring ∼ 300 nanotubes. The histogram shows that the nanotube diameters are dispersed from 0.7 to 6 nm with a broad peak at 1.3 nm. Besides individual SWNTs, we do observe other forms of nanotubes synthesized with the Fe_2O_3/alumina catalyst. First, bundles of SWNTs (Fig. 1a) are present, with each bundle containing a few tubes. The diameters of SWNTs within these bundles are also dispersed and range from ∼ 1 to 6 nm. Secondly, we do occasionally observe double-walled nanotubes in this material. From high-resolution TEM images, we have measured the diameters of the SWNT bundles and the observed double-walled nanotubes. Statistically, the smallest diameter of the bundles is ∼ 4 nm, and all of the double-walled nanotubes exhibit diameters larger than 2.5 nm. These results lead to the conclusion that in the AFM data, nanotubes that exhibit diameters less than 2.5 nm are mostly (> 90%) individual SWNTs. Also, we notice that the nanotubes examined by TEM appear free of amorphous coating and free of topological defects at least on the 1 μm length scale.

When using silica supported catalysts in methane CVD, we find that only bundles of SWNTs are synthesized. The SWNT bundles have diameters between 4 and 47 nm, and lengths up to tens of micrometers. In Fig. 3a,b respectively, we show typical low- and high-magnification TEM images of SWNT bundles produced by a Fe_2O_3/silica catalyst. The well-resolved and aligned fringes (Fig. 3b) suggest that the nanotubes are well packed in each bundle. High-magnification TEM images have allowed statistical measurements of the spacing between fringes in several bundles. We find that the spacing is constant within each bundle. By tilting our sample in the TEM, we do observe variation in the spacing between nanotube fringes in a given bundle. These results suggest that the individual SWNTs in a same bundle are nearly monodispersed in diameter.
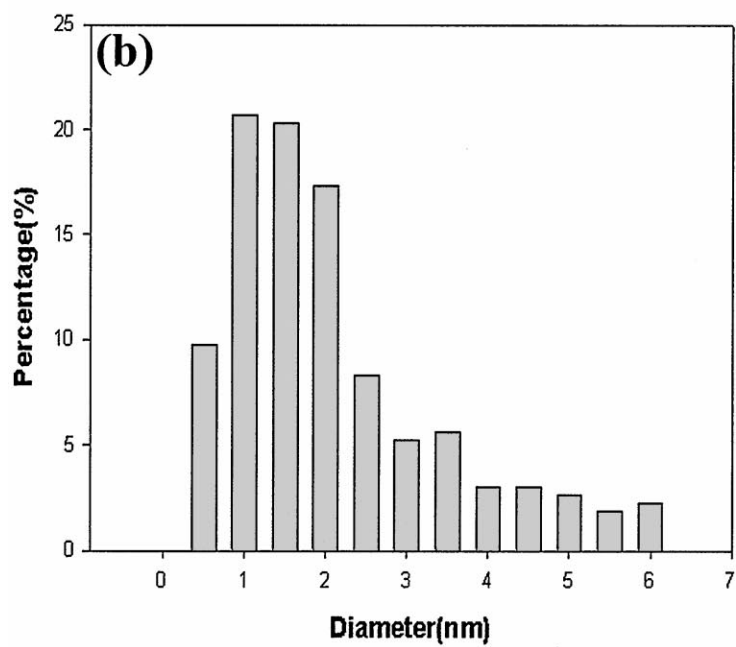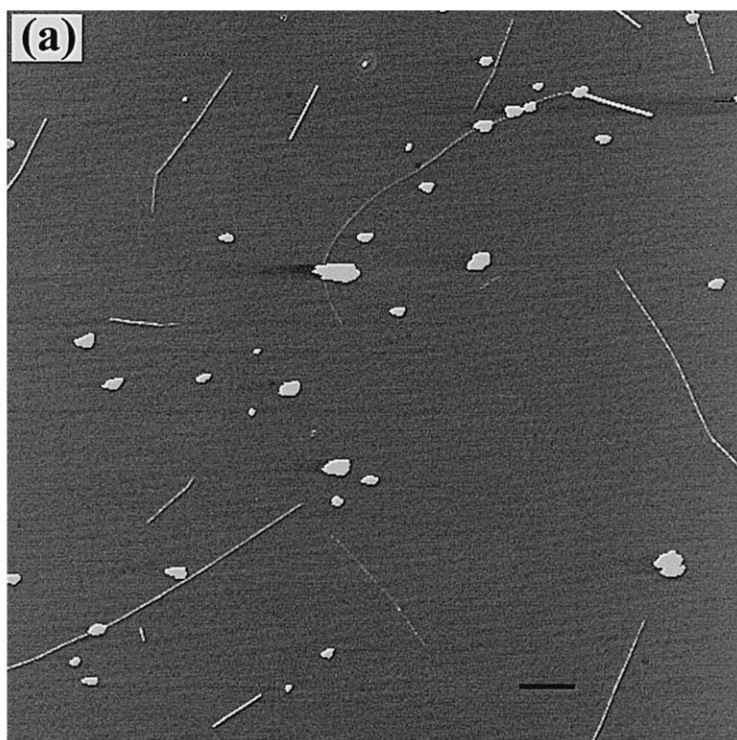
NiO, CoO and NiO/CoO catalysts are prepared by starting with $Ni(NO_3)_2 \cdot 6H_2O$, $Co(NO_3)_2 \cdot 6H_2O$, and a mixture of $Ni(NO_3)_2 \cdot 6H_2O/ Co(NO_3)_2 \cdot 6H_2O$, respectively. These catalysts in methane CVD have led to interesting but complex results. First, none of the NiO/alumina and NiO/silica catalysts produced SWNTs. Secondly, CoO and NiO/CoO catalysts produced SWNTs only on one of the alumina or silica supports (Table 1). Fig. 4a,b show TEM images of SWNTs synthesized on CoO/alumina, NiO/CoO/silica catalysts, respectively. In the material synthesized on the NiO/CoO/silica catalyst, we have observed only SWNT bundles. In contrast, small bundles and the occasional individual SWNTs are observed on the CoO/alumina catalyst. Thirdly, the yield of SWNTs appears much lower than the Fe_2O_3 catalysts. Currently, a quantitative measure of SWNT yield in our materials is lacking. Yield is only estimated by counting the number of nanotubes around a given volume of particles from TEM data.

4. Discussion

We believe that a number of variables in our CVD approach are key to the success of obtaining high-quality SWNTs. First, we chose methane as carbon feedstock at temperatures on the order of 1000°C. Methane is known to be the most kinetically stable hydrocarbon that undergoes the least pyrolytic decomposition at high temperatures. Therefore, the carbon atoms needed for nanotube growth are supplied by the catalytic decomposition of methane on transition metal surfaces. This is one of the main reasons that the synthesized nanotubes are nearly free of amorphous carbon coatings caused by self-pyrolysis of methane. Secondly, we limit CVD reaction times to ~ 10 min at a high methane flow rate to prevent amorphous carbon accumulation. Previous methane CVD syntheses of carbon fibers and multi-walled nanotubes have found and utilized the build-ing up of carbon over-coating to an appreciable thickness (sub-micrometer) over a time period of several hours near 1000°C temperatures [6,16,17]. Thirdly, so far, we find that supported Fe_2O_3 catalysts produces SWNTs much more efficiently than NiO, Co, and the NiO/Co mixture. Note that using X-ray photoelectron spectroscopy (XPS) on the catalyst made from $Fe(NO_3)_3 \cdot 9H_2O$ and heated to 1000°C for 5 min in argon, we have confirmed that the active catalyst composition is Fe_2O_3.

To understand the growth mechanism of SWNTs in the methane CVD process, we have carried out systematic TEM imaging of nanotube ends that are easily observable in our materials. In Fig. 1b (inset), we show a typical high-resolution TEM image of the end of an individual SWNT synthesized on the Fe_2O_3/alumina catalyst. With all of the materials listed in Table 1, we can only observe one end of a individual SWNT or a bundle. The other end is always found buried in particles. Furthermore, all of the ends that we have imaged so far appear closed and contain no metal particles.

Based on the states of the nanotube ends, we propose that SWNTs in our methane CVD processes grow via the 'base-growth' mechanism. Previously work on CVD synthesis of carbon fibers and nanotubes have found that the initial growth step involves absorption, decomposition of hydrocarbon molecules on a catalyst particle, and diffusion of carbon atoms into the catalyst bulk from a supersaturated catalyst surface [10,18,19]. We believe that this first step applies to our current process. However, the 'base-growth' model proposes that a nanotube lengthens with a particle-free closed-end, and carbon feedstock is supplied from the base where the other end of the nanotube interfaces with the catalyst material [10,18,20]. Thus, the 'base-growth' is the dominating growth mechanism for our SWNT materials. In contrast, the 'tip-growth' model proposes that a nanotube lengthens while carrying away a metal catalyst particle at its end [10,18,20]. The carried-along particle supplies the carbon feedstock

Fig. 2. (a) Tapping mode AFM image of carbon nanotubes produced on the Fe_2O_3/alumina catalyst. Z range (dark to bright): 4 nm. Scale bar: 0.5 μm. Sonication may have caused some of the short nanotubes [25]. (b) Diameter histogram of nanotubes determined from AFM data.
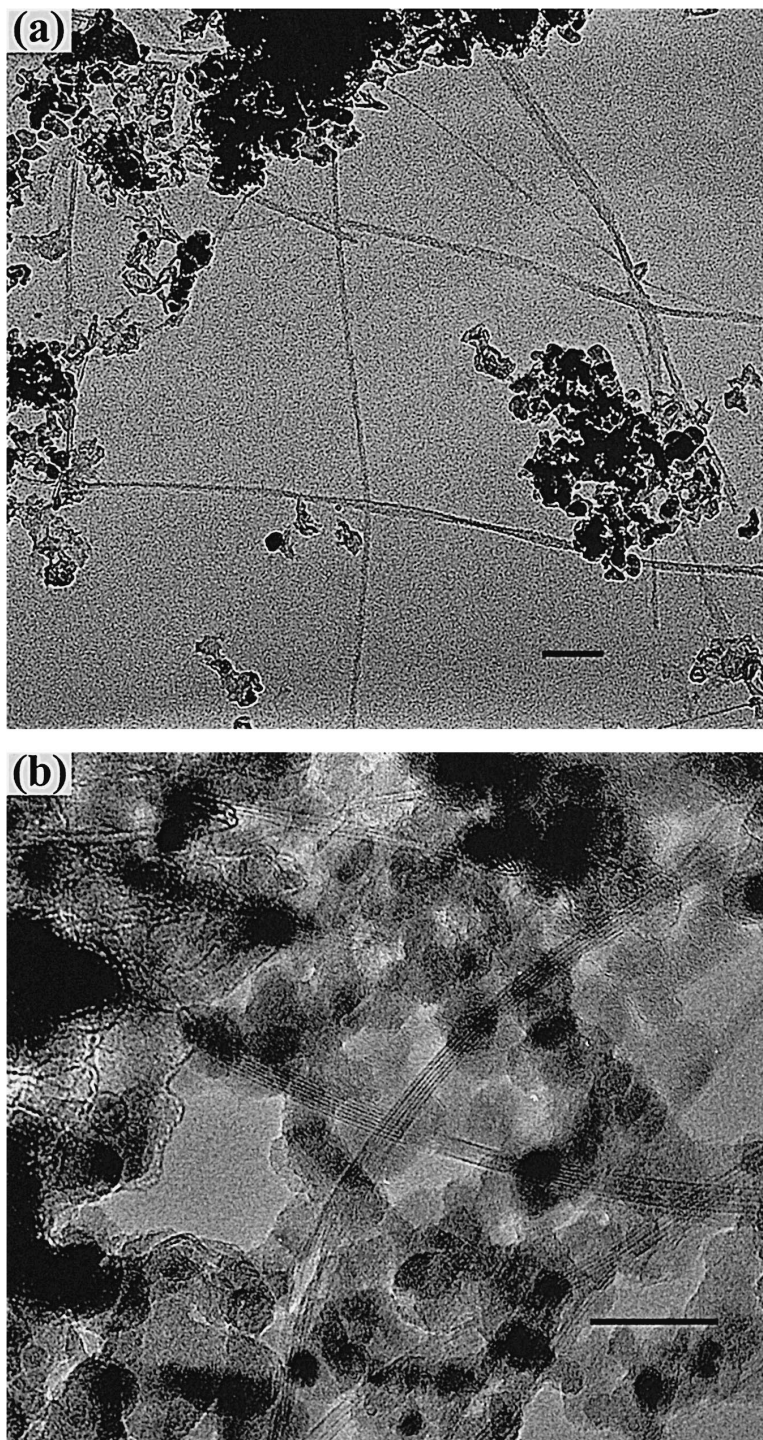
Fig. 3. (a) TEM image of SWNT bundles synthesized with the Fe_2O_3/silica catalyst. Scale bar: 100 nm. (b) High-resolution TEM image of SWNT bundles exhibiting fringes of individual SWNTs in the bundles. Scale bar: 50 nm.
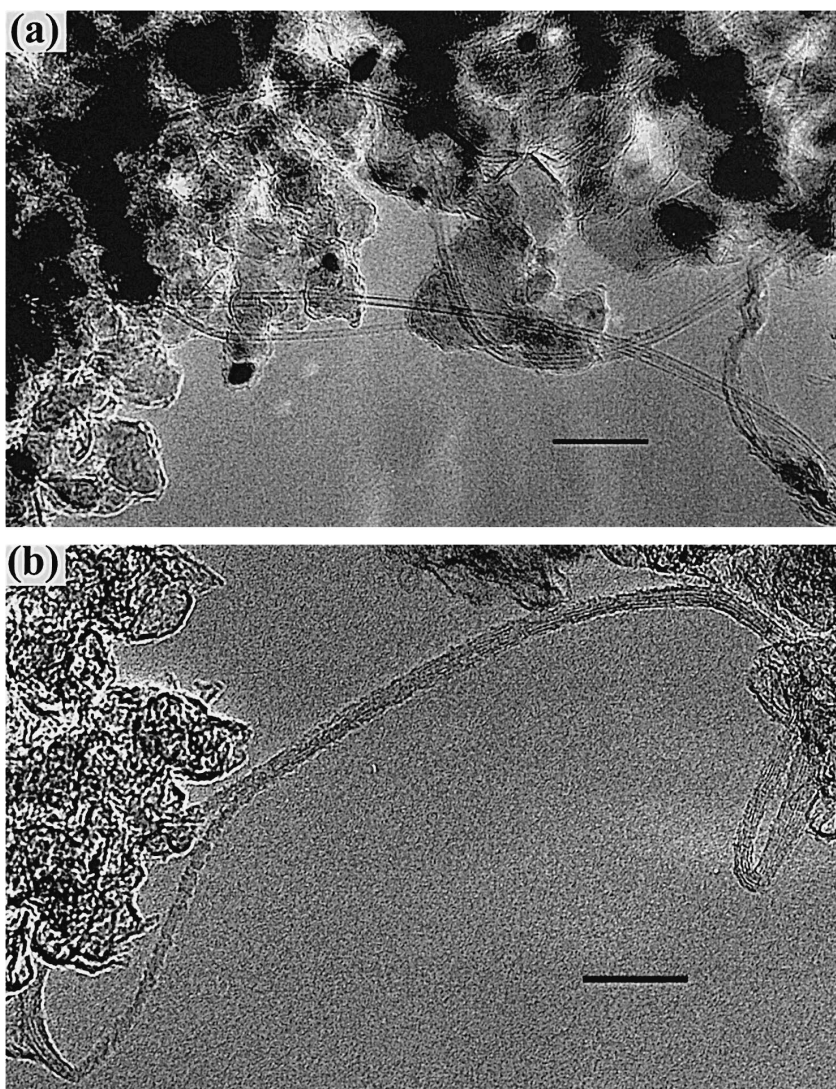
Fig. 4. (a) TEM image of SWNTs synthesized with the CoO/alumina catalyst. Scale bar: 25 nm. (c) TEM image of a SWNT bundle synthesized on the NiO/CoO/silica catalyst. Scale bar: 50 nm.

for growth. This 'tip-growth' mechanism does not apply to the current SWNT materials, since all the observed ends appear closed and particle-free. Nevertheless, we point out that, SWNTs synthesized in the CO–MoO$_x$ CVD approach [14] are results of 'tip-growth', since most of the observed nanotube ends do contain a metal nanoparticle [14].

The distribution of active catalytic particles on a support should dictate the type of SWNTs that are produced. As described earlier, the Fe$_2$O$_3$/alumina catalyst yielded abundant individual SWNTs, while the Fe$_2$O$_3$/silica catalyst yielded abundant SWNT bundles. We rationalize these results by considering the structures of the catalyst support materials. The fumed-alumina material consists of crystalline δ-form Al$_2$O$_3$ nanocrystals. [21] These nanocrystals are anisotropic since they contain crystal edges and corners. Therefore, different types of metal catalytic particles may form on the alumina particles. This leads to catalytic particles of varying sizes and distri-

butions, thus producing a mixture of tube types. In contrast, the fumed silica has an amorphous structure [22] and an isotropic surface. We believe that active catalyst particles on this isotropic support are uniformly and closely distributed. Therefore, the SWNTs nucleated on the close-by catalyst sites grow into bundles to maximize the van der Waals interactions between the walls of the nanotubes.

A detailed understanding of the different transition metal-oxide catalysts is currently lacking and requires future studies. We note that previously, Fe, Ni, Co, and mixed Ni/Co catalysts have all successfully produced SWNTs in laser-ablation and arc-discharge approaches [1–4,23,24]. Interestingly, in arc-discharge, SWNTs have been synthesized using Fe catalyst when methane is present in the discharge chamber [1]. Future work is also required to further explore (1) detailed pictures of nanotube growth as well as nucleation, (2) various catalyst compositions and concentrations, (3) new types of catalyst support, and (4) optimum growth conditions. The methane CVD approach could bring new possibilities to nanoscale science and technology.

Acknowledgements

References

[1] S. Iijima, T. Ichihashi, Nature 363 (1993) 603.
[2] A. Thess, R. Lee, P. Nikolaev, H.J. Dai, P. Petit, J. Robert, C.H. Xu, Y.H. Lee, S.G. Kim, A.G. Rinzler, D.T. Colbert, G.E. Scuseria, D. Tomanek, J.E. Fischer, R.E. Smalley, Science 273 (1996) 483.
[3] D.S. Bethune, C.H. Kiang, M.S. deVries, G. Gorman, R. Savoy, J. Vazquez, R. Beyers, Nature 363 (1993) 605.
[4] C. Journet, W.K. Maser, P. Bernier, A. Loiseau, M.L. Delachapelle, S. Lefrant, P. Deniard, R. Lee, J.E. Fischer, Nature 388 (1997) 756.
[5] S. Iijima, MRS Bull. 19 (1994) 43.
[6] G.G. Tibbetts, Appl. Phys. Lett. 42 (1983) 666.
[7] G.G. Tibbetts, Carbon 27 (1989) 745.
[8] G.G. Tibbetts, in Carbon Fibers, Filaments and Composites, Kluwer Academic, Amsterdam, 1990, p. 73.
[9] R.T.K. Baker, in: P. Walker, P. Thrower (Eds.), Physics and Chemistry of Carbon, Vol. 14, 1978, pp. 83.
[10] R.T.K. Baker, Carbon 27 (1989) 315.
[11] R.T.K. Baker, N.M. Rodriguez, Catalytic Growth of Carbon Nanofibers and Nanotubes, Symposium of the Materials Research Society, Materials Research Society, 1994.
[12] H.G. Tennent, Hyperion Catalysis International, USA, 1987.
[13] C.E. Snyder, W.H. Mandeville, H.G. Tennent, L.K. Truesdale, Int. Pat. WO 89/07163, 1989.
[14] H.J. Dai, A.G. Rinzler, P. Nikolaev, A. Thess, D.T. Colbert, R.E. Smalley, Chem. Phys. Lett. 260 (1996) 471.
[15] A. Fonseca, K. Hernadi, P. Piedigrosso, L.P. Biro, S.D. Lazarescu, P. Lambin, P.A. Thiry, D. Bernaerts, J.B. Nagy, Electrochem. Sci. Proc. 97–14, 1997, 884.
[16] H. Jaeger, T. Behrsing, Composites Sci. Tech. 51 (1994) 231.
[17] L.C. Qin, S. Iijima, Mater. Lett. 30 (1997) 311.
[18] G.G. Tibbetts, M.G. Devour, E.J. Rodda, Carbon 25 (1987) 367.
[19] G.G. Tibbetts, J. Cryst. Growth 66 (1984) 632.
[20] S. Amelinckx, X.B. Zhang, D. Bernaerts, X.F. Zhang, V. Ivanov, J.B. Nagy, Science 265 (1994) 635.
[21] Degusssa, Technical Bulletin N56.
[22] Degussa, AEROSIL: Fumed Silica.
[23] C.-H. Kiang, G. Wa III, R. Beyers, J.R. Salem, D.S. Bethune, J. Phys. Chem. 98 (1994) 6612.
[24] S. Seraphin, J. Electrochem. Soc. 142 (1995) 290.
[25] K.L. Lu, R.M. Lago, Y.K. Chen, M.L.H. Green, P.J.F. Harris, S.C. Tsang, Carbon 34 (1996) 814.